Supervised imitation learning of FS-MPC algorithm for multilevel converters

Novak, Mateja; Blaabjerg, Frede

Published in:
2021 23rd European Conference on Power Electronics and Applications (EPE'21 ECCE Europe)

Publication date:
2021

Document Version
Accepted author manuscript, peer reviewed version

Supervised imitation learning of FS-MPC algorithm for multilevel converters

Mateja Novak, Frede Blaabjerg

Department of Energy Technology, Aalborg University
Pontoppidanstræde 111
9220 Aalborg, Denmark
Email: nov@et.aau.dk, fbl@et.aau.dk

Acknowledgments

The work is supported by the Reliable Power Electronic-Based Power System (REPEPS) project at the Department of Energy Technology, Aalborg University as a part of the Villum Investigator Program funded by the Villum Foundation.

Keywords

≪Converter control≫, ≪Multilevel converters≫, ≪Neural networks≫, ≪Voltage Source Converter≫.

Abstract

Model predictive control (MPC) applications for multilevel power electronics converters are often facing problems of a high computation burden. By using supervised imitation learning, it is possible to synthesise computationally light controllers, which can capture the behaviour of computationally heavy MPC. To obtain a high performance controller, which can do the correct control actions, training data generation and pre-processing of the data are of high importance. This paper presents guidelines for training data generation and artificial neural network (ANN) controller design for a multistep-horizon finite set FS-MPC applied to neutral point clamped (NPC) converter. A particular challenge of the selected converter topology is that some control actions are used more often than others, thus the training data will be heavy skewed i.e. it will be difficult for the controller to learn when to apply these actions due to the lack of data. A workaround for solving this challenge is discussed in the paper. The performance and the robustness of the designed controller has been validated in a hardware in the loop (HIL) system, where the limitations of the synthesised ANN controller were explored. It was observed that ANN controller performance can match the performance of the FS-MPC algorithm when operating within the span of training data values and the computational burden was much lower.

Introduction

Artificial neural networks (ANN) have rapidly spread into various engineering applications. In power electronics applications, they are used to solve problems in design optimization [1,2], maintenance [3,4] and control [5,6] that go beyond the capabilities of the traditional methods [7]. One of the problems, where an ANN based solution was proposed, is the reduction of the high computational burden of multistep horizon FS-MPC for power electronic converters. Due to the iterative structure of the FS-MPC algorithm, an extension of the prediction horizon is exponentially increasing the number of required calculations. In [8,9] supervised machine learning is used to create a computationally light ANN controller that can provide a matching performance to the original FS-MPC controller. This reduces the need for a high speed control platform application or the use of sorting algorithms to reduce the number of

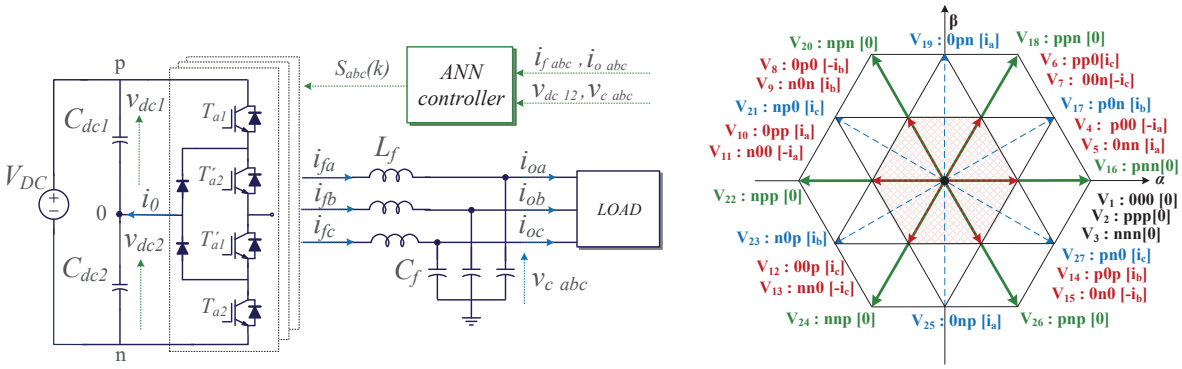

(a) Three phase 3L-NPC converter in standalone operation.

(b) Voltage vectors of the 3L-NPC converter and corresponding neutral point current (i_0).

Fig. 1: System schematics and voltage vectors of a 3L-NPC converter.

candidates that need to be evaluated. The next application that should be investigated is the supervised machine learning application in the multi-level converters, where a further increase of the FS-MPC computational burden is expected. In [10] four deep neural networks are employed to control the switches of a 5-level flying capacitor converter. This solution has a significant drawback, as the accuracy of the control depends on the accuracy of four septate neural networks. Moreover, it might not be necessary to employ such large network for this application.

Application of the imitation learning for multi-level converters presents a hidden challenge that was not addressed in [8, 9]. Both papers explore the applications in a two level voltage source converter where only 7 or 8 voltage vectors are utilized. In machine learning this is referred to as a classification problem [11] and it can be said that the input data is assigned to one of the 8 classes. It is expected that all vectors during normal operation of the converter are utilized equally. Thus, when generating the datasets for training the ANN controller, a balanced distribution of classes will be obtained. However, this does not apply for multilevel converter applications, where depending on the cost function design and operating conditions of the converter like commutation restrictions and modulation index, some voltage vectors will be utilized more often while others will be rarely applied. This leads to a very uneven distribution of classes, which requires application of techniques for imbalanced classification learning. Imbalanced classification is an open problem and it needs to be practically identified and addressed specifically for each training dataset [12, 13]. Therefore, the guidelines for the ANN application addressed in this paper can be of significant help for the future classification applications in power electronics. Moreover, in previous publications the limitations of the trained ANN controller were not explored i.e. can the network operate in the operating points that were not included in the training data? How high is the robustness of the trained network to model uncertainties? In [14] it was demonstrated that FS-MPC algorithm shows a high robustness to model parameter mismatch, the question is if this robustness is also inherited by the trained ANN controller. In the following section these questions will be answered by performing a HIL verification of the trained ANN controller.

System model

The FS-MPC application with highly unbalanced distribution of classes, which is addressed in this paper, is a three level neutral point clamped converter (3L-NPC) operating in a standalone application as shown in Fig. 1a. In Table I are summarized the converter system parameters. In the 3L-NPC converter 27 voltage vectors like depicted in Fig. 1b can be selected by the FS-MPC algorithm and applied to the converter output. It can be observed that small voltage vectors ($V_5 - V_{14}$) and medium voltage vectors ($V_{17}, V_{19}, V_{21}, V_{23}, V_{25}, V_{27}$) control the neutral point current flow (i_0), thus their application is important for obtaining a balanced neutral point (NP) voltage. Predictions of system voltages and currents are calculated using the following differential equations in the αβ reference frame:

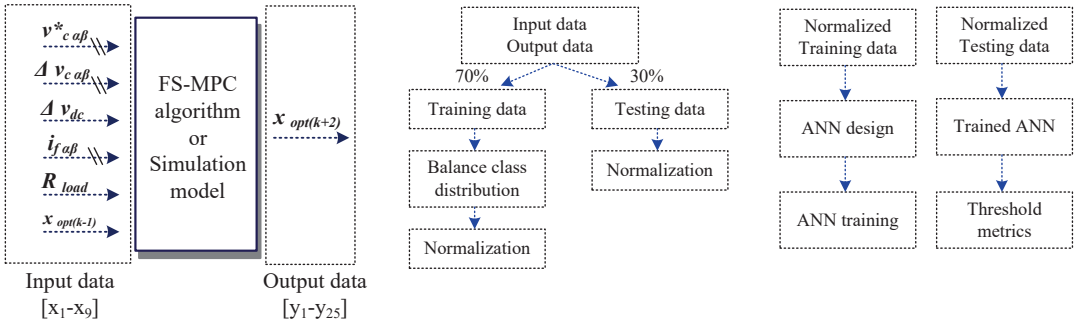

Fig. 2: Training data generation, preprocessing and ANN training to be applied in 3L-NPC converter.

$$v_{dc1,2}(t) = C_{dc1,2}\frac{di_{dc1,2}(t)}{dt} \quad i_{f\alpha\beta}(t) = C_f\frac{dv_{c\alpha\beta}(t)}{dt} + i_{o\alpha\beta}(t) \quad v_{i\alpha\beta}(t) = L_f\frac{di_{f\alpha\beta}(t)}{dt} + v_{c\alpha\beta}(t) \quad (1)$$

where $v_{dc1,2}$ are the DC-link voltages, $C_{dc1,2}$ are the capacitances of the DC-link capacitors and $i_{dc1,2}$ are the capacitor currents, i_f is the filter current and v_c is the filter capacitor voltage which also corresponds to the load voltage, L_f and C_f are output filter inductance and capacitance and v_i is the inverter output voltage. To reduce the cost of the system, a state observer was implemented to estimate the load current as shown in [15, 16]. The cost function implemented in the FS-MPC algorithm has two objectives: voltage reference tracking, where $v^*_{c\alpha,\beta}$ are reference voltages and $v^P_{c\alpha,\beta}$ the predicted voltages, and NP voltage balancing, which minimizes the voltage difference of the two DC-link capacitors:

$$g = (v^*_{c\alpha} - v^P_{c\alpha})^2 + (v^*_{c\beta} - v^P_{c\beta})^2 + \lambda_{dc}(v^P_{vdc1} - v^P_{dc2})^2 \quad (2)$$

Although it is not used in this example, switching frequency minimization can also be implemented like shown in [8]. Without switching frequency minimization the number of utilized voltage vectors is reduced to 25. If the prediction horizon is extended to 2, the number of possible voltage vector combinations that need to be evaluated by the algorithm will reach 625 combinations. In the following section, guidelines for generating the training data and techniques for preprocessing the data will be presented. The goal of the ANN controller is to learn the control principles of the 2-step horizon FS-MPC controller.

Training data generation

The quality of the training data has a high impact on the trained ANN accuracy. Two approaches for data generation can be distinguished: simulation based data generation [8, 10] and artificial dataset created by defining the input variable state-space and afterwards used as inputs for the FS-MPC algorithm [9].

Data generation from simulation model

The downside of collecting the data from the simulation model is that it requires more time and it is difficult to extensively cover the state-space of the input variables. Transients are one of the phenomena that are not easy to cover. Moreover, in case a current limitation is included in the cost function, the simulation based data generation needs to cover the cases where the limiter is activated in order to learn how to apply the switching states that can keep the converter in a safe operation mode.

Artificial data set

Generating the artificial dataset is faster and it can cover a much wider input variable space state. It is very important to analyse the behaviour of the converter system to correctly specify the input variable state space. This can be done by observing the simulation results of the converter system with the original FS-MPC algorithm. For example it can help to identify the average, maximum and minimum value of the

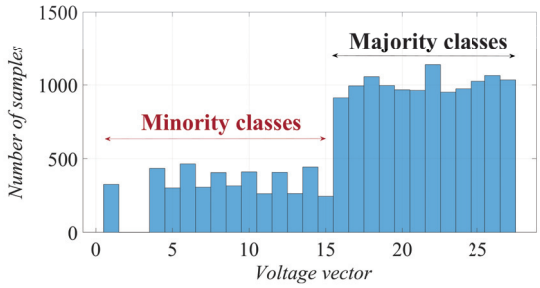

(a) Voltage control, DC-link balancing.

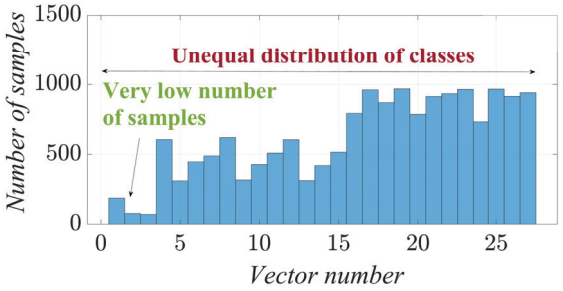

(b) Voltage control, DC-link balancing and switching frequency minimization.

Fig. 3: Voltage vector (class) distribution recorded during operation of 3L-NPC converter for different objectives in the cost functions of FS-MPC algorithm.

inputs. This will help in correctly defining the span of the inputs and whether it makes sense to uniformly sample this span or increase the density of the samples close to the minimum value. One downside of the artificial data set is that once the input vector range is defined and used to create a mash grid with all possible combinations of these vector values, it is possible to get a lot of combinations that are less likely to appear in normal operation conditions. Therefore, the accuracy of the trained ANN might be lost by the ANN trying to fit these ambiguous datasets.

Class distribution

As mentioned in the introduction, learning the behaviour of the FS-MPC algorithm applied to power converters represents a classification problem where the output vectors of the converter are defined as classes. It needs to be mentioned that most of the machine learning algorithms are optimized for application on cases with a balanced class distribution i.e. all classes have approximately the same number of data samples. In multilevel converters like the NPC converters, the problem of unbalanced classes as shown for example in Fig. 3 will emerge. Unbalanced class distribution is very often observed in many classification problems like e.g the fraud detection, spam detection, anomaly detection [12] etc. where there is one minority class and one majority class. The application presented in this paper will have to deal with not only one minority and majority class, but multiple, making the complexity of recognising the correct class even tougher.

In the first step of II. Data preprocessing (see Fig. 2), it is important that the class distribution is preserved when the data set is split to training data and testing data. The test data should preserve the imbalance, as this imbalance will also be present in the operating conditions of the controller. Next, techniques for correcting the skewness of the class distribution in the training dataset need to be applied. This can be done either by under-sampling the majority classes or oversampling the minority classes. In most cases it was proven that a combination of both methods can provide good results. Another alternative is cost-sensitive learning where to each class a different misclassification cost is applied to correctly or incorrectly classified samples. Thus, misclassification of a minority class will have a higher cost value. The goal here is to minimize the total misclassification cost [17]. Several combinations of oversampling and under sampling were applied to the training artificial training data generated for the 3L-NPC converter applications. The highest accuracy improvement was obtained for combination of SMOTE (Synthetic minority oversampling technique) and ENN (Edited nearest neighbours rule). SMOTE selects a random data point of a minority class and then finds its k nearest neighbours from the same class, a random neighbour is selected and a synthetic example is created between the two examples in the feature space. The procedure is repeated until the number of minority class samples has reached the desired number. Afterwards, ENN is using the k=3 nearest neighbours to locate examples that are misclassified and deletes them. The purpose of the ENN is to find ambiguous and noisy examples in a dataset. After improving the class distribution, the ANN input training data and ANN input testing data are normalized separately in order to avoid data leakage. The output training and testing data are encoded using the one-hot encoding technique as shown in [9].

Table I: Parameters of the converter system .

Parameter	Value
DC-link voltage (V_{DC})	520 V
DC-link capacitors ($C_{dc1,2}$)	4 mF
Filter inductance (L_f)	2.4 mH
Filter capacitance (C_f)	15 μF
Reference ($V_c^*, f_{v_c}^*$)	230 V, 50 Hz
Sampling time (T_s)	25 μs

Table II: Input training data range.

Input variable	Range
Filter current ($I_{f\alpha\beta}$)	[-9:3:9] A
Load voltage error ($\Delta v_{c\alpha\beta}$)	[-6:1.5:6] V
Load resistance (R_{load})	[30:10:60] Ω
DC-link imbalance (Δv_{dc})	[-1:0.25:1] V
Voltage reference ($V_{c\alpha\beta}^*$)	[-230:44:230] V
Previously applied vector (x_{old})	[1:1:25]

For the selected case study of a 2-step horizon controller, 39 million data points were initially generated in step I depicted in Fig. 2. The range of the input data is summarized in Table II. 13 minority classes corresponding to zero vector and all small vectors (see Fig. 1b) were identified. The ratio of number of samples in minority classes and majority classes was 6:100, indicating a high skewness of the class distribution. Therefore, the mentioned methods for correcting the skewness of the class distribution were applied. If this step is skipped, the synthesized controller would not have enough samples to learn when to apply the small and zero vectors, which as mentioned before are essential for NP balancing of the NPC converter.

Neural network design

Neural network design is an iterative process. A good starting point is to define a network with one hidden layer that has a number of neurons that is higher than the number of neurons in the input and output layer. In the application presented in this paper the input layer has 9 neurons ($x_1, x_2 ... x_9$) and the output layer 25 neurons ($y_1, y_2 ... y_{25}$). Thus, for the hidden layer 30 neurons were chosen. If after the training the accuracy of the network is not sufficient, the number of neurons can be increased or a second hidden layer can be added. A rectifier linear unit (ReLU) was used as the activation function (f_1) for the hidden layer and a softmax activation function (f_2) for the output layer as shown in Fig. 4. Optimization algorithm Adam was used to update the weights (w_n) and bias (b_n) parameters of the ANN.

Output of the n-th neuron in the hidden layer:

$$h_n = f_1(b_{n1} + \sum_{j=1}^{9} w_{nj}^{(1)} \cdot x_n)$$

Output of the y-th neuron in the output layer:

$$y_n = f_2(b_{n2} + \sum_{k=1}^{30} w_{nk}^{(2)} \cdot h_n)$$

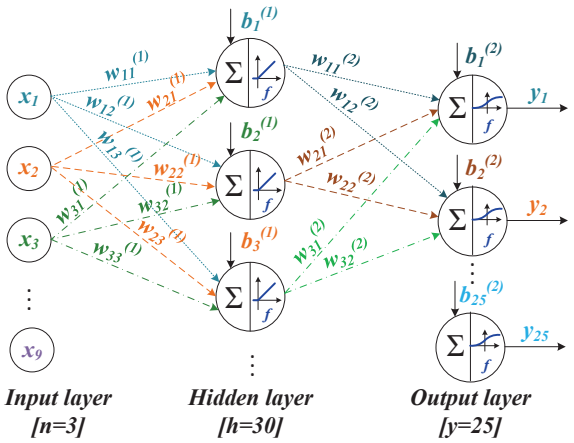

Fig. 4: Structure of the feed-forward ANN used in the case study. Number of input neurons n=9, hidden layer neurons h=30 and output neurons y=25.

The data preprocessing and training of the network were performed in Python using the machine learning libraries (keras, tensorflow, scikit-learn, imbalanced-learn etc.) on a workstation with 12 processor cores to reduce the required training time to 20 minutes. To monitor the performance of the ANN training, classification accuracy can not be used as it is not an appropriate metrics for imbalanced classification. Instead, following threshold metrics that are most commonly used for imbalanced classification were defined: categorical accuracy, F1 score, recall score and precision. Precision score quantifies the number of minority class samples that belong to minority class and recall score quantifies how well the minority

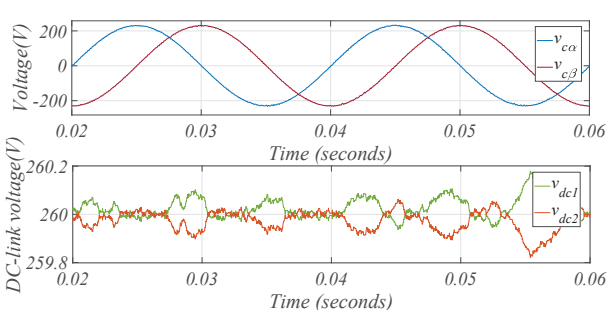

(a) Waveforms for the original 2-step prediction FS-MPC controler (THD=0.77%, f_{sw}= 7.1 kHz).

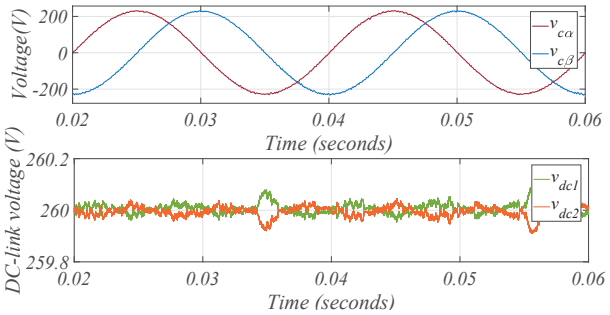

(b) Waveforms for the ANN controller (THD=0.88%,f_{sw}= 6.8 kHz).

Fig. 5: Output voltage waveforms in αβ reference frame and DC-link voltage balancing performance of 3L-NPC converter with two controllers.

classes were predicted [12]. The F1 score is obtained as a combination of precision and recall score. For the application presented in the paper 88% categorical accuracy was obtained during the validation phase of the ANN.

Performance evaluation

After the successful training, the obtained ANN can be implemented in MicroLab controller to check the required computational time. The turn around of the trained ANN with a sampling time of T_s = 25 μs was 21 μs, while the FS-MPC algorithm due to the high number of iterative calculations (625 iterations) required 47 μs and produced an overrun. As it was not possible to safely operate the converter system with a 2-step FS-MPC algorithm and T_s = 25μs, a benchmark performance comparison will be done using the Simulink models. In Fig. 5 the simulated waveforms of the load voltage and DC-link capacitor voltages can be observed for the two controllers. A very good reference tracking and balancing can be observed by the ANN controller. Moreover, the total harmonic distortions (THD) of the load and the operating switching frequencies of the controllers show only 11% and 4% difference. This confirms the very high accuracy of the ANN controller. For a comparison, the ANN controller that was trained on the data that used only random majority class under sampling (a number of samples in the majority class was randomly selected and then removed from the dataset) was also implemented in the 3L-NPC converter system. The obtained waveforms showed the load voltage THD of 1.3%, a switching frequency of 5.7 kHz. However, instabilities in the NP balancing were observed. This means that the controller did not successfully learn the behaviour of the original FS-MPC controller.

Hardware in the loop validation

The synthesized ANN controller was implemented in dSpace MicroLab box. A detailed converter system model as shown in Fig. 1 was created and downloaded to the Typhoon HIL 404 platform which provides a safe environment for testing the robustness of the controller and exploring its limitations. The first conducted test, as shown in Fig.7 was the steady state performance test of the voltage control and NP balancing. The obtained results were in accordance with the simulations, showing low THD and good balance of the NP. Afterwards, a step load change from 60 Ω to 30 Ω, which is within the range of training data, was performed. A fast current response can be observed and a minimum voltage sag at the moment of the load change, see Fig. 8.

Next, operating points that are out of range of the training data were tested. First the load resistance was decreased to 15 Ω. From the obtained voltage waveforms in Fig. 9 it can be noticed that the system has provided a stable response, with a good NP balance but the reference was not correctly traced. There is a noticeable 30V drop in the voltage amplitude. In contrary, when the load resistance was increased to 70 Ω in Fig. 10, where there was no significant drop in the voltage amplitude and the NP balance was also

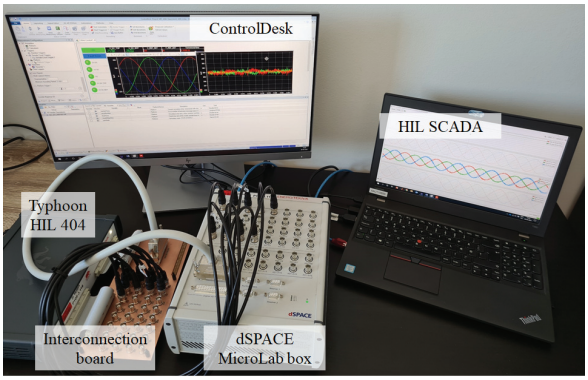

Fig. 6: HIL set-up for validation of the ANN controller performance and robustness.

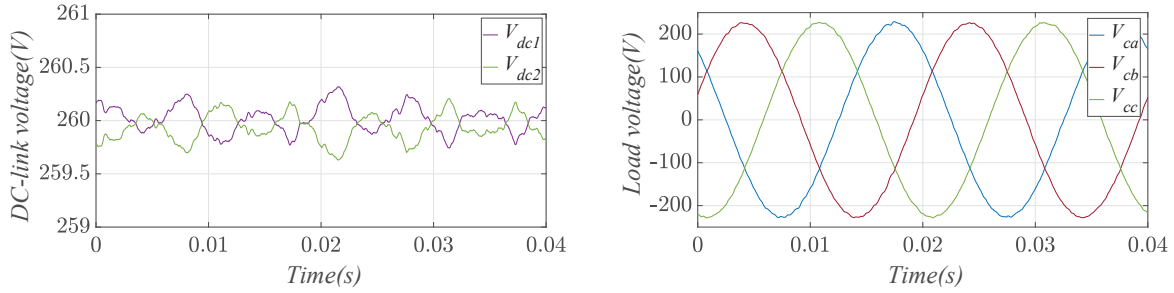

(a) DC-link voltages. (b) Load voltages (THD = 0.99%).

Fig. 7: Voltage waveforms of a 3L-NPC converter with 2-step ANN controller for R_{load}=30 Ω, V_{ref} = 230V, V_{dc} = 520V obtained in HIL system.

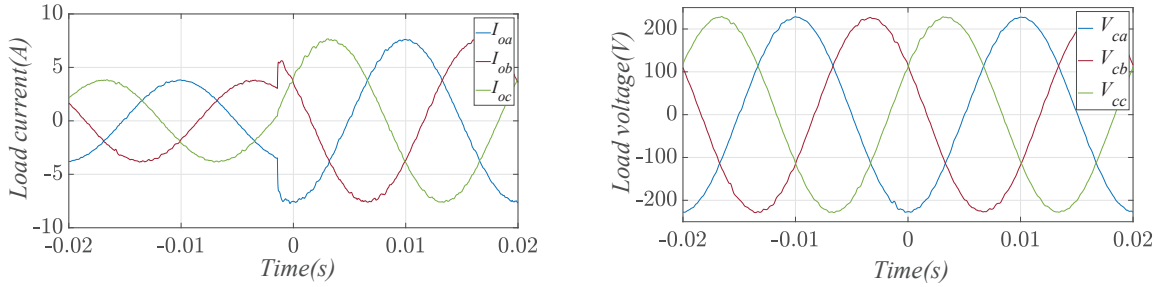

(a) Load currents. (b) Load voltages.

Fig. 8: Step response of a 3L-NPC converter with 2-step ANN controller for R_{load}=60 → 30 Ω, V_{ref} = 230V, V_{dc} = 520V obtained in HIL system.

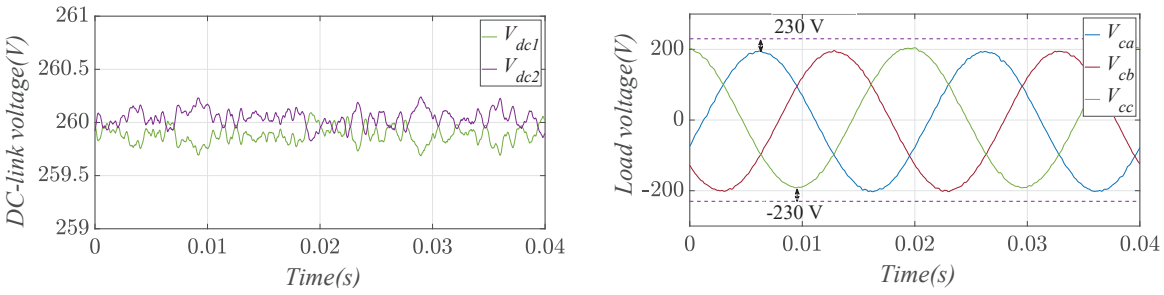

(a) DC-link voltages. (b) Load voltages (THD = 1.17%).

Fig. 9: Voltage waveforms of a 3L-NPC converter with 2-step ANN controller for R_{load}=15 Ω, V_{ref} = 230 V, V_{dc} = 520 V obtained in HIL system.

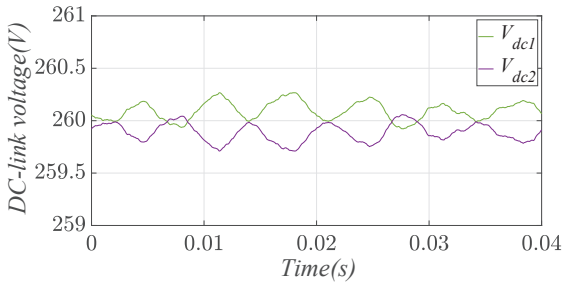

(a) DC-link voltages.

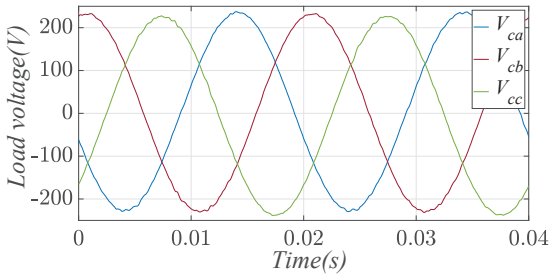

(b) Load voltages (THD = 1.17%).

Fig. 10: Voltage waveforms of a 3L-NPC converter with 2-step ANN controller for R_{load}=70 Ω, V_{ref} = 230 V, V_{dc} = 520 V obtained in HIL system.

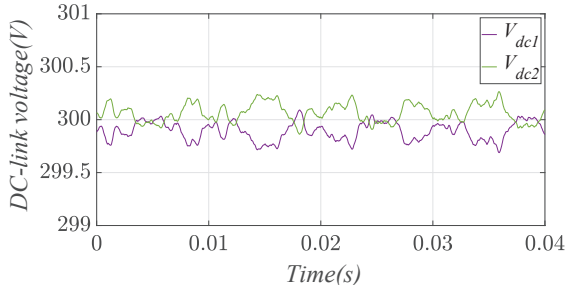

(a) DC-link voltages.

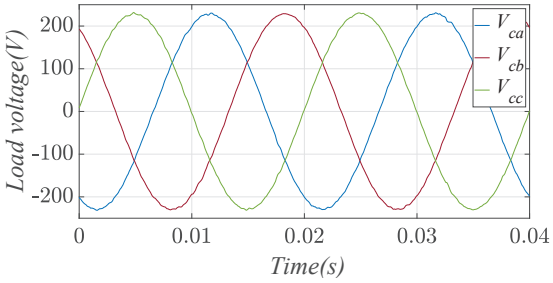

(b) Load voltages (THD = 1.11%).

Fig. 11: Voltage waveforms of a 3L-NPC converter with 2-step ANN controller for R_{load}=30 Ω, V_{ref} = 230 V, V_{dc} = 600 V obtained in HIL system.

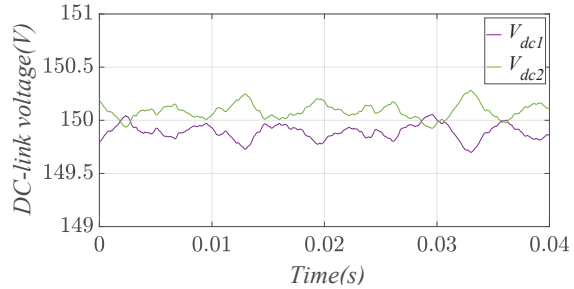

(a) DC-link voltages.

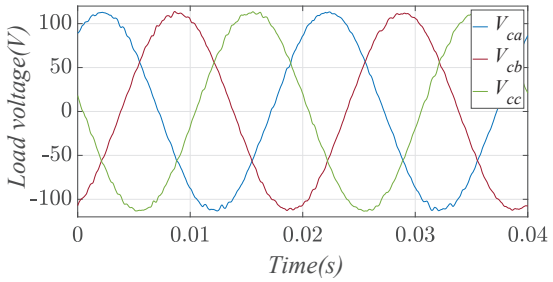

(b) Load voltages (THD = 1.6%).

Fig. 12: Voltage waveforms of a 3L-NPC converter with 2-step ANN controller for R_{load}=30 Ω, V_{ref} = 120 V, V_{dc} = 300 V obtained in HIL system.

retained. Therefore, to increase the span of the controller operating points the load range of the training data should be expanded to include the low values.

Another system variable that is interesting to evaluate in the robustness validation is the DC-link input voltage. Two cases were defined, one with a higher voltage (V_{dc} = 600 V), shown in Fig. 11, and lower voltage (V_{dc} = 300 V), shown in Fig. 12. For the second, the reference was reduced to 120V. In both operating points the controller provided a stable response and NP balance.

In the final test the controller robustness to parameter mismatch was tested. Interestingly, the controller responded well to the negative mismatch of the values i.e. the values of the LC filter that were used in training were 30% smaller than the one set in the HIL simulator. However, for positive mismatch the controller could not provide the correct response. This indicates that in order to have a controller that is robust to parameter mismatch, the training would have to be modified to also include these data points.

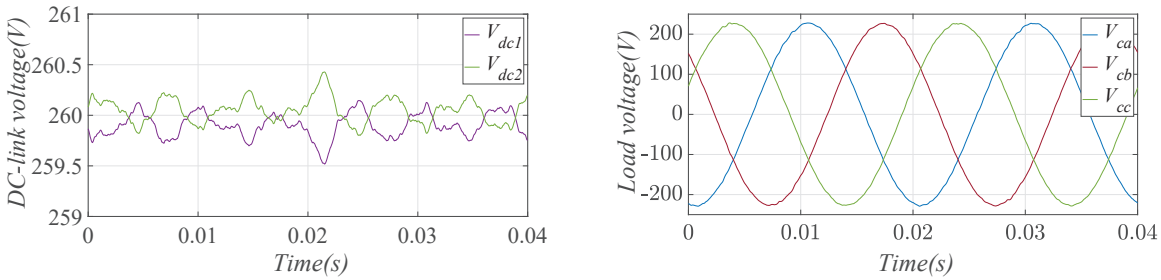

(a) DC-link voltages.

(b) Load voltages (THD = 1.12%).

Fig. 13: Voltage waveforms of a 3L-NPC converter with 2-step ANN controller for R_{load}=30 Ω, V_{ref} = 230 V, V_{dc} = 520 V and 30% filter parameter mismatch obtained in HIL system.

Table III: Summary of the ANN controller tests in HIL system.

System parameters values	Response	THD(V_c)
Within training range	stable	0.99%
R_{load} = 15 Ω	stable	1.17%
R_{load} = 70 Ω	voltage sags	1.17%
V_{dc} = 115% $V_{dc\,nom}$	stable	1.11%
V_{dc} = 60% $V_{dc\,nom}$	stable	1.60%
L_f = 130% $L_{f\,nom}$ C_f = 130% $C_{f\,nom}$	stable	1.12%
L_f = 70% $L_{f\,nom}$ C_f = 70% $C_{f\,nom}$	unstable	-

Conclusion

ANN can be used for implementation of high computational FS-MPC algorithms in multilevel power electronic converters. In the presented example of a 3L-NPC converter, 2-step horizon FS-MPC algorithm can be replaced by a shallow ANN, which is executed 2 times faster than the conventional FS-MPC algorithm implementation without a significant accuracy loss. However, in order to achieve a high accuracy of the ANN, the training data should be balanced and provide good coverage of the operating states of the converter. With a correct preprocessing of the training data, the difference in the performance metrics (THD and the NP balancing) of the trained ANN controller and the FS-MPC controller were within 11%. The ANN controller responded well to DC-link voltage values which were out of the training range. It was also discovered that the ANN controller does not have a high robustness to parameter mismatch and load values out of training range. Thus, to improve this, training data should also include response to mismatched parameters and higher load value span.

References

[1] T. Wu, Z. Wang, B. Ozpineci, M. Chinthavali, and S. Campbell, "Automated heatsink optimization for air-cooled power semiconductor modules," *IEEE Trans. Power Electron.*, vol. 34, no. 6, pp. 5027–5031, 2019.

[2] B. Zhao, X. Zhang, and J. Huang, "AI algorithm-based two-stage optimal design methodology of high-efficiency CLLC resonant converters for the hybrid ACDC microgrid applications," *IEEE Trans. Ind. Electron.*, vol. 66, no. 12, pp. 9756–9767, 2019.

[3] B. Hu, Z. Hu, L. Ran, P. Mawby, C. Jia, C. Ng, and P. McKeever, "Deep learning neural networks for heat-flux health condition monitoring method of multi-device power electronics system," in *In Proc. IEEE Energy Conversion Congress and Exposition (ECCE)*, 2019, pp. 3769–3774.

[4] B. Yang, R. Liu, and E. Zio, "Remaining useful life prediction based on a double-convolutional neural network architecture," *IEEE Trans. Ind. Electron.*, vol. 66, no. 12, pp. 9521–9530, 2019.

[5] X. Fu, S. Li, M. Fairbank, D. C. Wunsch, and E. Alonso, "Training recurrent neural networks with the levenbergmarquardt algorithm for optimal control of a grid-connected converter," *IEEE Trans. Neural Networks and Learning Systems*, vol. 26, no. 9, pp. 1900–1912, 2015.

[6] G. Book, A. Traue, P. Balakrishna, A. Brosch, M. Schenke, S. Hanke, W. Kirchgssner, and O. Wallscheid, "Transferring online reinforcement learning for electric motor control from simulation to real-world experiments," *IEEE Open Journal of Power Electron.*, vol. 2, pp. 187–201, 2021.

[7] S. Zhao, F. Blaabjerg, and H. Wang, "An overview of artificial intelligence applications for power electronics," *IEEE Trans. Power Electron.*, vol. 36, no. 4, pp. 4633–4658, 2021.

[8] I. Hammoud, S. Hentzelt, T. Oehlschlaegel, and R. Kennel, "Long-horizon direct model predictive control based on neural networks for electrical drives," in *In Proc. 46th Annual Conference of the IEEE Industrial Electronics Society (IECON)*, 2020, pp. 3057–3064.

[9] M. Novak and T. Dragicevic, "Supervised imitation learning of finite-set model predictive control systems for power electronics," *IEEE Trans. Ind. Electron.*, vol. 68, no. 2, pp. 1717–1723, 2021.

[10] D. Wang, X. Yin, S. Tang, C. Zhang, Z. J. Shen, J. Wang, and Z. Shuai, "A deep neural network based predictive control strategy for high frequency multilevel converters," in *In Proc. IEEE Energy Conversion Congress and Exposition (ECCE)*, 2018, pp. 2988–2992.

[11] M. A. Nielsen, *Neural Networks and Deep Learning*. Determination Press, 2015.

[12] J. Brownlee, *Imbalanced Classification with Python: Better Metrics, Balance Skewed Classes, Cost-Sensitive Learning*. Machine Learning Mastery, 2020.

[13] A. Fernandez, S. Garcia, M. Galar, R. C. Prati, B. Krawczyk, and F. Herrera, *Learning from Imbalanced Data Sets*. Springer, Cham, 2018.

[14] M. Novak, U. M. Nyman, T. Dragicevic, and F. Blaabjerg, "Statistical performance verification of FCS-MPC applied to three level neutral point clamped converter," in *In Proc. 20th European Conference on Power Electronics and Applications (EPE'18 ECCE Europe)*, 2018, pp. P.1–P.10.

[15] P. Cortes and J. Rodriguez, "Three-phase inverter with output LC filter using predictive control for UPS applications," in *In Proc. 2007 European Conf. on Power Electron. and Appl.*, 2007, pp. 1–7.

[16] B. Majmunovic, T. Dragicevic, and F. Blaabjerg, "Multi objective modulated model predictive control of stand-alone voltage source converters," *IEEE Journal of Emerging and Sel. Topics in Power Electron.*, vol. 8, no. 3, pp. 2559–2571, 2020.

[17] H. He and Y. Ma, *Imbalanced Learning: Foundations, Algorithms, and Applications*, 1st ed. Wiley-IEEE Press, 2013.